A MODIFIED HARMONIC-BALANCE ANALYSIS OF SCHOTTKY DIODE MULTIPLIERS BASED UPON A HYDRODYNAMIC TRANSPORT MODEL

C. C. Lee[1], B. L. Gelmont[3], D. L. Woolard[2] and C. Fazi[1]

U.S. Army Research Laboratory
[1]RF & Electronics, Adelphi, MD 20783
[2]Army Research Office, RTP, NC 27709

[3]The University of Virginia
Electrical Engineering Department
Charlottesville, VA 22903

Abstract

The accurate design and successful implementation of very high frequency nonlinear circuits requires both a detailed understanding of the physical operation of the active devices and of how these nonlinear devices interact with the linear embedding circuit. This work addresses the specific task of establishing a robust simulation tool that can be used to for the future design of GaAs Schottky diode multipliers at terahertz ($\sim$ 0.3-10.0 THz) frequencies. This paper will present an entirely new algorithm for the optimization of these combined multiplier elements. In this novel approach, the available second-harmonic power of the diode is first optimized over all allowable diode excitation voltages and harmonics.

I. INTRODUCTION

It is well known that energy-transport effects become important above approximately 300 GHz, where the oscillation period becomes comparable to the intrinsic energy relaxation time in GaAs ($\sim$ 3 picoseconds). Hence, the accurate modeling of the electron dynamics within reversed- or forward-biased GaAs Schottky diodes, even in the lower portion of the terahertz frequency band, requires the incorporation of a hydrodynamic, or energy-transport, approach. The specific focus of this paper is on energy transport effects and their influence on the harmonic multiplication within reversed-bias Schottky-barrier varactor diodes. Equally important to the characterization of diode multipliers is the optimization of the nonlinear element to the externally coupled embedding impedance. Here, the second-harmonic power (i.e., current and voltage) of the matched diode is optimized before constraints on embedding impedance, local voltage and dc bias are specified. The key of this approach is the reduction of systems variables by an efficient mathematical ordering of the optimization procedure. Specifically, this new method reduces the typical optimization problem (i.e., where device and circuit are considered simultaneously) for a doubler, where 2 harmonics are considered, from n+2 variables to n variables. As will be shown, this approach leads to a significant computational advantage for Schottky-diode multiplier design.

In this paper, a one-dimensional time-dependent simulation algorithm is presented which employs a fully hydrodynamic transport model (i.e. first three moments of the Boltzmann equation) to describe the diode physics within the depletion and bulk regions. These preliminary studies consider diode operation in the lower portion of the terahertz band (i.e. < 1 THz) where electron momentum relaxation is not a factor. These studies assume a reversed-biased situation and employ appropriate boundary conditions at the barrier interface. Specifically, boundary conditions include an energy-dependent constraint on the thermionic-emission current and an energy-dependent constraint on the energy-flow density. In addition, this work combines the physically accurate diode model with a

modified harmonic-balance algorithm to determine diode-circuit designs that maximize power generation and/or power efficiency in the second harmonic. The modified harmonic-balance method utilizes a novel two-step procedure where the available doubler-power and the second-harmonic diode-impedance is first derived as a function of first and second harmonic diode excitation. The harmonic diode-voltages and second-harmonic diode-impedance at the optimum power-point are then used define the matched embedding impedance and the optimum local-oscillator (LO) voltage. Note that the optimum values for both the direct and alternating components of the LO source are derived. The utility of this simulation tool is illustrated by comparing to prior studies, by others, that employed traditional drift-diffusion transport models, Monte Carlo transport models and a conventional harmonic-balance algorithm. Specifically, this work demonstrates a computationally efficient and accurate physical description as well as a more robust approach for circuit optimization.

II. PHYSICS-BASED DIODE MODEL

These multiplier studies utilize a physics-based Schottky-diode model accurate for both momentum and energy relaxation effects. Here, a one-dimensional time-dependent simulation algorithm is implemented that employs a fully hydrodynamic transport model (i.e. first three moments of the Boltzmann equation) to describe the diode physics within the depletion and neutral regions. The application this type of approach will be necessary for GaAs diodes operating at terahertz frequencies because energy relaxation is important above 300 GHz (i.e., since $\tau_w \approx 3.0 \times 10^{-12}$ seconds) and momentum relaxation is important above 1 THz (i.e. since $\tau_m \approx 0.25 \times 10^{-12}$ seconds). While our method is fully amenable to momentum relaxation these initial studies will consider device operation below 1 THz and the explicit time-dependence on current density (i.e., momentum) in the momentum balance equation will be suppressed for computational convenience. These studies consider the large-signal operation of a Schottky-barrier varactor frequency multiplier and will therefore consider diodes under time-dependent reverse-bias up to the breakdown voltage. Hence, these studies assume a reversed-biased situation and employ traditional boundary conditions at the barrier interface. Specifically, boundary conditions include an energy-dependent constraint on the thermionic-emission current and an energy-dependent constraint on the energy-flow density.

Hydrodynamic Transport Model

The electron-transport model equations used here are similar to that in [1]. Specifically, the time-dependent hydrodynamic model used in this study conserve electron density, n, electron charge-flux, $\bar{J}_n$, and average electron energy, w_n, according to

$$q\frac{\partial n}{\partial t} - \nabla \cdot (\bar{J}_n) = 0, \tag{1}$$

$$\bar{J}_n = qD_n\nabla n + n\mu_n(k_B\nabla T_e - q\nabla\psi). \tag{2}$$

$$\frac{\partial(nw_n)}{\partial t} + \nabla \cdot \bar{S}_n = -\bar{J}_n \cdot \nabla\psi + n(\frac{\partial w_n}{\partial t})_c, \tag{3}$$

and derives self-consistent, ψ, potentials from Poisson's equation

$$\nabla \cdot (\varepsilon \, \nabla \psi) = q(n - N_D).$$ (4)

Here, q is the free electron charge, D_n is the diffusion coefficient, μ_n is the electron mobility, k_B is the Boltzmann constant, T_e is the electron-gas temperature, $\bar{S}_n$ is the electron energy-flux density, ε is the electric permittivity and N_D is the donor concentration. The diffusion coefficient is determined from the generalized Einstein relation

$$D_n = \frac{\mu_n k_B T_e}{q}$$ (5)

The electron energy flow $\bar{S}_n$ is given by

$$\bar{S}_n = -\kappa_n \nabla T_e - (w_n + k_B T_e) \frac{\bar{J}_n}{q}.$$ (6)

The thermal conductivity κ_n is related to the mobility μ_n by the Wiedmann-Franz law

$$\kappa_n = (\frac{5}{2} + c) q n \mu_n (\frac{k_B}{q})^2 T_e,$$ (7)

where c is an adjustable parameter, taken here to be −1/2. The average electron energy w_n is defined using the usually thermal approximation (i.e., drift component ignored)

$$w_n = \frac{3}{2} k_B T_e.$$ (8)

The collision terms are modeled by the relaxation-time approximation. The energy collision term in (3) is expressed as

$$(\frac{\partial w_n}{\partial t})_c = -\frac{w_n - w_0}{\tau_w},$$ (9)

where $w_o = 3 k_B T_o / 2$ is the equilibrium energy at the lattice temperature T_o and τ_w is the energy relaxation time. In this work, a constant relaxation time, $\tau_w = 3$ ps, has been utilized [1]. The diffusion coefficient is defined from the generalized Einstein relation (5) where a general mobility with a temperature dependence is assumed. For free particle path-lengths much less that the epitaxial layer width, the mobility dependence on electric field. $F = -\nabla \psi$. can be approximated by [1]

$$\mu_n(F) = \frac{\mu_0 + v_{sat} \cdot F^3 / F_0^4}{1 + (F / F_0)^4} \tag{10}$$

where μ_0 is the low-field, doping-dependent mobility, v_{sat} is the saturation velocity and F_0 is the critical electric field. Here, $v_{sat} = 1.5 \times 10^5$ m/s and $F_0 = 4.0 \times 10^5$ V/m has been utilized. The doping-dependent mobility is given by

$$\mu_0 = \frac{\mu_{00}}{1 + [\log(N_T) / B]^n} \tag{11}$$

where N_T is the total doping density (here total ionization is assume so $N_T = N_D$). Here, $\mu_{00} = 0.838$ m²/V-s, $n = 23$, and $B = 23.26$ are used for GaAs. A temperature-dependent mobility may be obtained by requiring the energy transport equation in the spatially homogeneous bulk to be consistent with the empirical field dependent mobility. Specifically, the energy-balance equation for a spatially homogeneous semiconductor yields

$$q\mu_n(F)F^2 = \frac{3}{2} \frac{k_B (T_e - T_0)}{\tau_w} \tag{12}$$

which can be solved self consistently with Eq. (10) to determine mobility as a function T_e. The previous model was utilized in this work to incorporate the effects of electron energy into the time-dependent operation of a reverse-bias Schottky varactor embedded into an arbitrary tuning network. A consistent and physically accurate set of boundary conditions will now be presented.

Boundary Conditions at the Schottky and Ohmic Contacts.

The accurate implementation of the hydrodynamic model to diode operation requires that an appropriate set of boundary conditions be applied to the device. Here, we will consider the case where a reverse bias is maintained on the diode during large signal operation. It is also important to note that the boundary conditions used in the physical devices must be applied at the ohmic-contact (i.e., at $z = L$, where L is the diode epitaxial length) and on the semiconductor-side of the Schottky-contact (i.e., at $z = 0^+$). In this investigation, conditions on the electron potential, electron density and electron temperature were enforced at both contacts. Here, nonlinear, mixed boundary conditions [1] were employed at the Schottky-contact to allow for nonequilibrium variations in density and energy. These boundary conditions are physically accurate and reasonable for reverse-bias diode operation, see discussion in [2].

The potential applied to the diode is defined in terms of the shift in the Fermi-energy between the Schottky-contact and the ohmic-contact. Hence, if $\psi(L)$ is used to denote the potential energy at the conduction-band edge of the ohmic-contact then the electron potential at the semiconductor-side of the Schottky contact is given by

$$\psi(0^+) = \psi(0^-) - \phi_b = \psi(L) - \phi_b - E_{F0} + V_D. \qquad (13)$$

where V_D is the diode applied bias, ϕ_b is the metal-semiconductor barrier height and E_{F0} is the difference between the Fermi-energy and the conduction band edge at the ohmic contact. The potential at the ohmic-contact $\psi(L)$ is used as the reference voltage and is kept constant during a simulation

The electron concentration at the ohmic-contact is assumed to be in dynamic equilibrium with the reservoir and therefore specified as

$$n(L) = N_D \qquad (14)$$

The carrier concentrations at the Schottky-contact are determined from Sze's thermionic-diffusion theory [1]. The electron concentration is defined dynamically from the electron exchange between metal and semiconductor. Here, the relative recombination velocity for electrons in the semiconductor, v_S, and in the metal, v_M, are employed. Hence, the thermionic-emission current of electrons across the metal-semiconductor boundary is expressed as

$$J_{TE}(0^+) = q(v_S\, n(0^+) - v_M\, n_M) \qquad (15)$$

where $n(0^-)$ is the electron concentration in the semiconductor at the interface and n_M is the electron concentration in the metal with energy enough to reach the conduction band of the semiconductor. This electron concentration is given by

$$n_M = N_C \exp(-\frac{\phi_B}{k_B T_e}). \qquad (16)$$

where N_C is the effective density of states. A hemi-Maxwellian distribution at the interface is use to approximate the electron recombination velocity in the semiconductor as

$$v_S = \sqrt{k_B T_e(0^+)/\pi m_n}\,, \qquad (17)$$

and in the metal as

$$v_M = \sqrt{k_B T_0/\pi m_n}\,, \qquad (18)$$

where, T_0 is the lattice temperature.

The electron energy, or electron temperature, at the ohmic-contact is assumed to be in dynamic equilibrium with the reservoir and therefore specified as

$$T_e(L) = T_0 \qquad (19)$$

The condition on electron temperature, at the Schottky-contact, is determined such that the energy crossing the boundary, derived from a recombination velocity model, is consistent with the energy-flux terms of the physical model. Here, energy carried by electrons passing from metal-to-semiconductor is balanced against energy carried by electrons passing from semiconductor-to-metal to derive the phenomenological energy-flux boundary condition [1]

$$S_n(0^+) = v_M \, n_M \, \delta \, k_B \, T_0 - v_S \, n(0^+) \delta \, k_B \, T_e(0^+), \tag{20}$$

where $\delta = 2$ is used. The hydrodynamic electron transport model was solved subject to the previous boundary conditions to provide a physically accurate description for Schottky-diode varactor operation.

III. VARACTOR FREQUENCY-MULTIPLIER NUMERICAL SIMULATION

Harmonic-Balance Technique

While an accurate model for the physical diode is very important as one attempts to design varactor multipliers at very high frequencies, the ability to effectively couple the device to the proper embedding impedance is of paramount importance. In fact, the majority of the analytical and numerical effort involved in realizing efficient multipliers is expended in the matching of the nonlinear device to the embedding circuit [3]. For example, many harmonic-balance methods have been derived (e.g., accelerated fixed point [4] and multiple reflection algorithm [5]) to improve the matching of the various harmonics between nonlinear device and linear circuit. Here the difficulty lies in the large number of iterations that are required to optimize power-efficiency of a given nonlinear element over both embedding impedance and local oscillator (LO) voltage. This problem becomes compounded for optimization over the physical diode design and in circuits that contain many nonlinear device elements [6]. Of course, in some situations where multiple diodes are involved equivalent-circuits can be developed that reduce groups of diodes to a single nonlinear element.

When a conventional harmonic-balance (HB) algorithm is applied to the analysis of a varactor-doubler the problem is to optimize the second-harmonic generation. Here, embedding impedances are selected for the first- and second-harmonic circuits and short-circuit conditions are assumed at the higher harmonics. While there are many HB techniques one of the most popular is the multiple reflection algorithm [5] that seeks to smooth transients via the introduction of a loss-less transmission-line section. This relaxation method, which in some cases requires long convergence times, has been improved by Tait [4]. Regardless of the exact mathematical algorithm employed, the primary challenge in the design of a doubler is to determine the embedding impedance that will yield the maximum second-harmonic power. In the conventional approach, the physical model of the Schottky diode is used in conjunction with the HB algorithm to optimize the second-harmonic power. Specifically, the HB technique will iterate between the Fourier-domain solutions of the circuit(s) and the current/voltage harmonics derived from steady-state time-domain simulations of the diode. Since this combined Fourier-domain and time-domain analysis inevitably leads to extensive iterations and to a large computational cost, it is natural to seeks alternative methods that reduce the numerical burden of the optimization task. In the simulations presented here, a new two-step procedure has been utilized to achieve this goal. This modified HB algorithm introduces a

new optimization constraint that enables a natural separation of the device-circuit problem. Specifically, this procedure allows the current/voltage harmonics of the nonlinear device to be optimized independently of the external circuit. Subsequently, the optimum embedding circuit can then be derived from a very simple analysis.

The key to this simplified approach is to formulate the optimization-problem of the varactor-doubler in a completely different way. Specifically, to recognize that the available-power of the diode at the doubler-frequency may be optimized a priori (i.e., independent of the external circuit) and that the Fourier results can be used, subsequently, to determine the embedding impedance and LO voltage. While this technique represents, in a manner of speaking, a inverse transformation of the conventional problem, it is completely valid and offers definite computational advantages. The technique is outlined in the text that follows. Invoking the normal assumptions that the nonlinear diode-element of a doubler experiences first- and second-harmonic voltage excitation, it is possible to express the total instantaneous voltage across the diode as

$$V_D(t) = -|V_{D0}| + V_{C1}\cos(\omega\,t) + V_{C2}\cos(2\omega\,t) + V_{S2}\sin(2\omega\,t) \tag{21}$$

where, ω, is the fundamental angular frequency and $|V_{D0}|$, V_{C1}, V_{C2} and V_{S2} is the dc, first, and second harmonic voltages, respectively. Note, the absence of the first sine-harmonic is completely general in that one only needs a specific time-reference point. The assumption that these harmonics are *known* and presented to the diode, only require that we assume that the first- and second-harmonic embedding impedances are matched and that the higher-harmonics are subject to an short-circuit. While a traditional HB algorithm is able to treat arbitrary embedding impedances, these imposed conditions are ones that are optimal for the final design. Hence, they are completely consistent with an optimization of the varactor-doubler. The main goal of the technique now is to maximize either (1) the second harmonic power available from the diode, or (2) the overall efficiency of diode-doubler. The first-harmonic power delivered to the diode is,

$$P_1 = V_{C1}I_{C1}/2, \tag{22}$$

and the available second-harmonic power from the diode is

$$P_2 = -(V_{C2}I_{C2} + V_{S2}I_{S2})/2. \tag{23}$$

The simple relations given in Eqs. (22) and (23) can now be used to optimize multiplier operation. The first step in the problem is to maximize either P_2, or P_2/P_1, over the four-dimensional space $(V_{D0}, V_{C1}, V_{C2}, V_{S2})$. Here, the current harmonics I_{C1}, I_{C2}, and I_{S2} are supplied by Fourier transforms of time-domain simulations from the physical diode model according to

$$I_D(t) = I_{D0} + \sum_{k=1} \{I_{Ck}\cos(k\omega t) + I_{Sk}\sin(k\omega t)\}. \tag{24}$$

Note that this new approach offers an immediate reduction in problem complexity as compared to the conventional HB approach. Specifically, the traditional HB method will maximize the nonlinear diode-circuit problem over LO voltage (dc and ac) and over the real and imaginary parts of the first- and second-harmonic embedding impedance which is a six-dimensional space. It should be noted that this reduction from N to N-2 in the

double problem also occurs in the analysis of a varactor-tripler due to symmetry considerations.

Once the optimization over diode-voltages has been completed. the matching embedding impedances are easily determined from

$$R_1 = 2P_1 / (I_{C1}^2 + I_{S1}^2),$$ (25)

$$X_1 = -R_1 I_{S1} / I_{C1},$$ (26)

$$R_2 = 2P_2 / (I_{C2}^2 + I_{S2}^2),$$ (27)

$$X_2 = (V_{S2} I_{C2} - I_{S2} V_{C2}) / (I_{C2}^2 + I_{S2}^2).$$ (28)

The final step to the procedure is to derive the optimum LO voltage. Shifting the time reference-point again (i.e., by θ) so that the fundamental harmonic of LO voltage only depends cosine leads to

$$V_D(t) = -|V_{D0}| + V_{C1} \cos(\omega t - \theta) + V_{C2} \cos(2\omega t - 2\theta) + V_{S2} \sin(2\omega t - 2\theta)$$ (29)

where

$$(\cos\theta, \sin\theta) = (I_{C1}, -I_{S1}) / \sqrt{I_{C1}^2 + I_{S1}^2}$$ (30)

The total LO voltage is now given by

$$V(t) = V_O + V_{LO} \cos(\omega t)$$ (31)

where

$$V_{LO} = 2R_1 \sqrt{I_{C1}^2 + I_{S1}^2},$$ (32)

$$V_O = I_O R_O - |V_{DO}|.$$ (33)

Here, the real impedance of the dc bias circuit is R_O and I_O is the dc diode current. Figure 1 summarizes the major differences between the conventional HB technique and the modified approached discussed here. As shown, the traditional HB technique requires two iterations. For each mapping over the six-dimensional LO-impedance space, one must perform convergent iteration to balance the harmonics between the embedding impedance and the nonlinear device. On the other hand, the modified method invokes allowable constraints on the available diode power and the embedding impedance(s) (i.e., are always matched to the diode impedance) to reduce the optimization space by two variables. Furthermore, the method requires a trivial calculation in the second step to derive the final impedance(s) and the LO voltage. In simplest terms reducing the degrees of freedom allows for a significant reduction in computation.

Conventional-Doubler
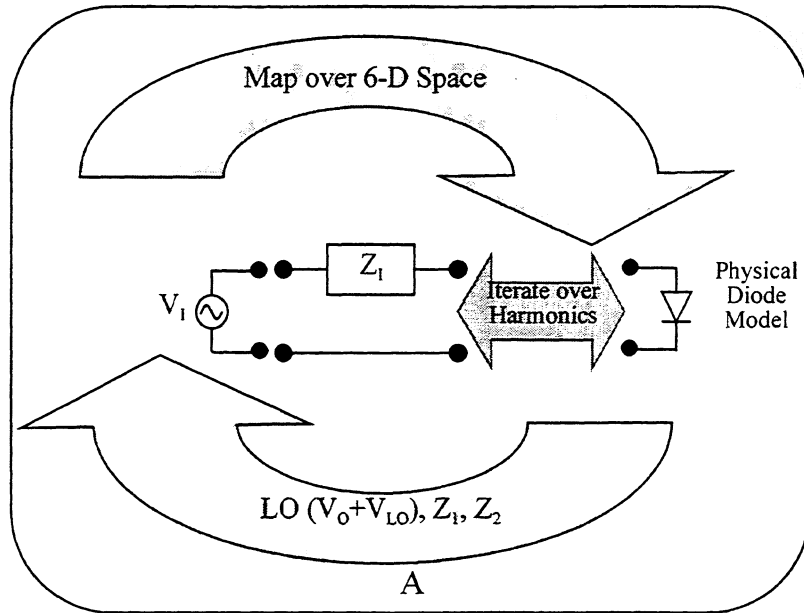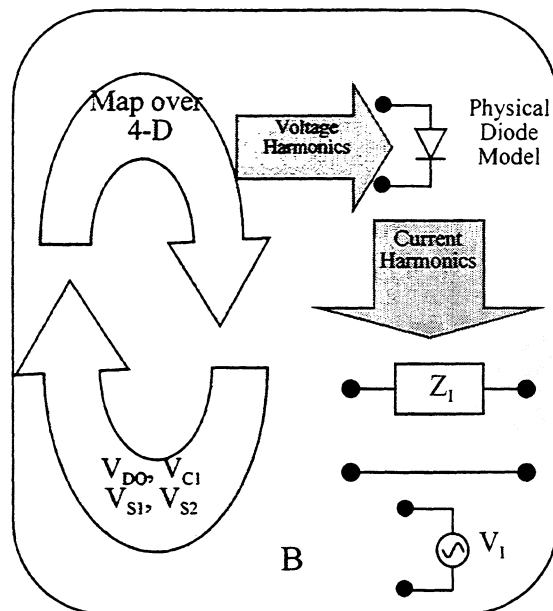

Modified-Doubler

Figure 1. Comparison of harmonic-balance schemes. (A) The conventional-doubler approach requires a map over six system variables and iterations for the harmonic-balance. (B) The modified-doubler only requires a map over four system variables and no balance iterations.

Simulation Results

The modified harmonic-balance approach was utilized with the hydrodynamic diode model to study Schottky diode multiplier operation at a doubler-frequency of 200 GHz. Here, the earlier varactor diode investigations that were presented in [7] were considered for comparison purposes. The GaAs Schottky diode considered was a UVA-6P4 with an epitaxial doping density of $n_D \approx 3.5 \times 0^{16}\,\text{cm}^{-3}$, epitaxial thickness of 1.0 μm, anode diameter 6.3 μm, series resistance 9.5 ohms and a breakdown voltage of 20 volts. The earlier studies in [7] were based upon a drift-diffusion diode-model. Hence, the studies presented here utilized both a simple depletion-region physical model and the hydrodynamic model presented in the last section.

The depletion-region (DR) diode model is based upon the familiar abrupt-junction approximation width depletion layer with w and neutral region width L-w. The thermionic emission current J_{TE} follows directly from Eqs. (15) and (16) and may, for the nondegenerate conditions considered here, be expressed as [8]

$$J_{TE} = q v_{mo} N_c \exp(-\frac{\phi_B}{k_B T_e})[\exp(\frac{q V_{bi}}{k_B T} - \frac{q^2 N_d w^2}{2\varepsilon k_B T}) - 1].$$

(34)

The total particle and displacement current density for the diode is therefore given by

$$J_D = J_{TE} - q N_D \frac{\partial w}{\partial t}.$$

(35)

The system of equations resulting from application of the DR model to the diode are [9]

$$\frac{J_D L}{q \mu_o N_d} = V_D - V_{bi} + \frac{q N_d w^2}{2\varepsilon}$$

(36)

$$\frac{dw}{dt} + \frac{\mu_o}{L}(V_D - V_{bi} + \frac{q N_d w^2}{2\varepsilon}) - \frac{J_{TE}}{q N_d} = 0$$

(37)

where ε is the permittivity, μ_0 is the low-field mobility and V_{bi} is the built-in potential. The DR model was utilized to provide an initial guess for the hydrodynamic simulator and for comparing to the final optimized results. The DR model and the modified harmonic-balance algorithm were used to estimate the optimum second-harmonic power of the Schottky-diode multiplier. The location this optimal power point in harmonic-space (i.e., V_{D0}, V_{C1}, V_{C2}, V_{S2}) was then used to define a new neighborhood for the hydrodynamic-based simulation algorithm. The hydrodynamic diode model simulator was used to generate the second-harmonic power map given in Fig. 2. Here, the second-harmonic power is mapped over the space (V_{C2}, V_{S2}) at the optimal values V_{D0} = 8.6, and V_{C1} = 9.0. The results indicate the strongest dependence on V_{C2}.

Power versus Second Harmonics
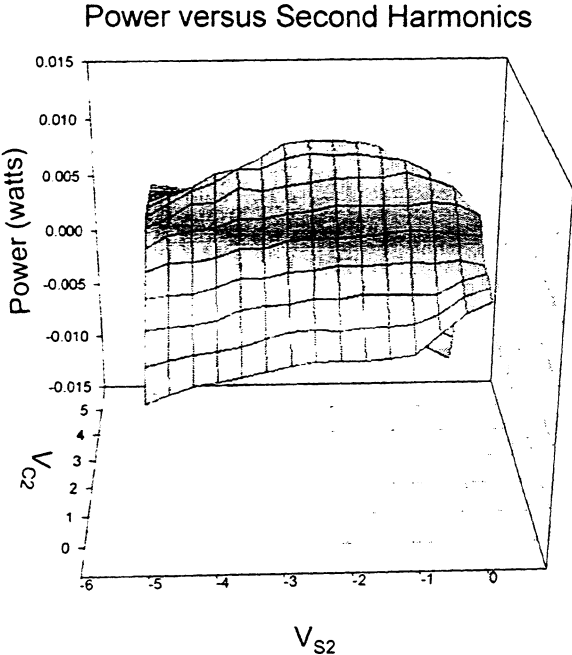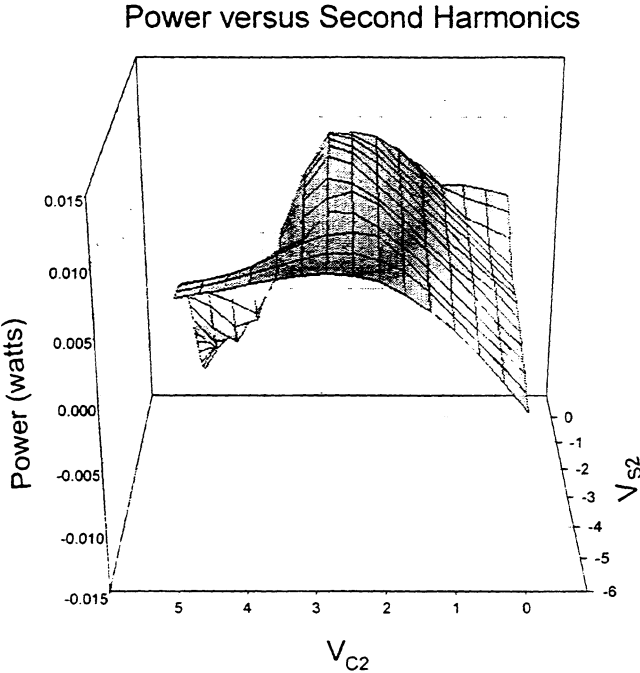

Power versus Second Harmonics

Figure 2. Second-Harmonic power versus second-harmonic voltages. Here, two perspectives are given to clearly show the variation along V_{C2} and V_{S2}.

The optimized results obtained from the hydrodynamic-based model are very close to the results from the DR model as shown in Table I-A. The very good agreement between both power and efficiency from the two models is not surprising since the frequency is much below the terahertz regime. These conclusions are further substantiated by the time-dependent results derived from the hydrodynamic model for electron charge-density and electron temperature given in Fig 3. As shown, the regular variation in the depletion-region edge (i.e., shown by the time-contour in Fig 3 (A)) and the nominal heating outside the depleted region are consistent with the assumptions of the simple DR model. The results are also in good agreement with the optimal power results, derived from the Monte Carlo transport model in reference [7]. These results are given in Table I-B. The discrepancy in the power results derived from the drift-diffusion model It is important to note that the results

Table I-A

Hydrodynamic Model with Modified HB		Depletion-Region Model with Modified HB	
Second Harmonic Power (mW)	P_{out}/P_{in} (%)	Second Harmonic Power (mW)	P_{out}/P_{in} (%)
13.03	60.34	12.57	57.06

Table I-B

MCHB simulator		DDHB simulator with weighted average a.c. mobility	
Second Harmonic Power (mW)	P_{out}/P_{in} (%)	Second Harmonic Power (mW)	P_{out}/P_{in} (%)
11.8	25.1	17.36	36.9

Table II-A

Hydrodynamic Model with Modified HB		Depletion-Region Model with Modified HB	
Z_1	Z_2	Z_1	Z_2
34+j251	41+j111	35+j253	40+j113

Table II-B

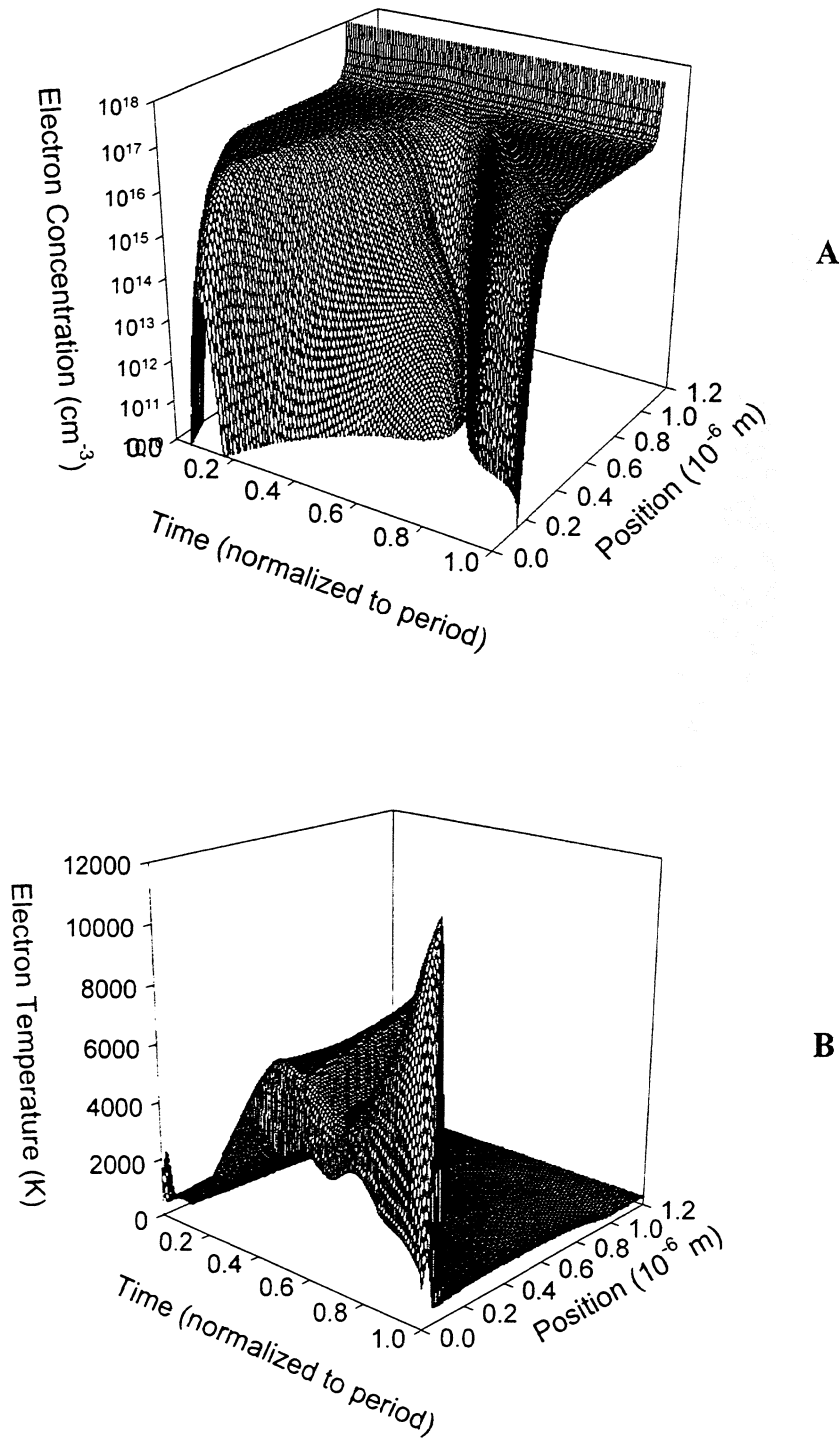| MCHB simulator		DDHB simulator with weighted average a.c. mobility	
Z_1	Z_2	Z_1	Z_2
62+j249	60+j128	39+j232	42+j117

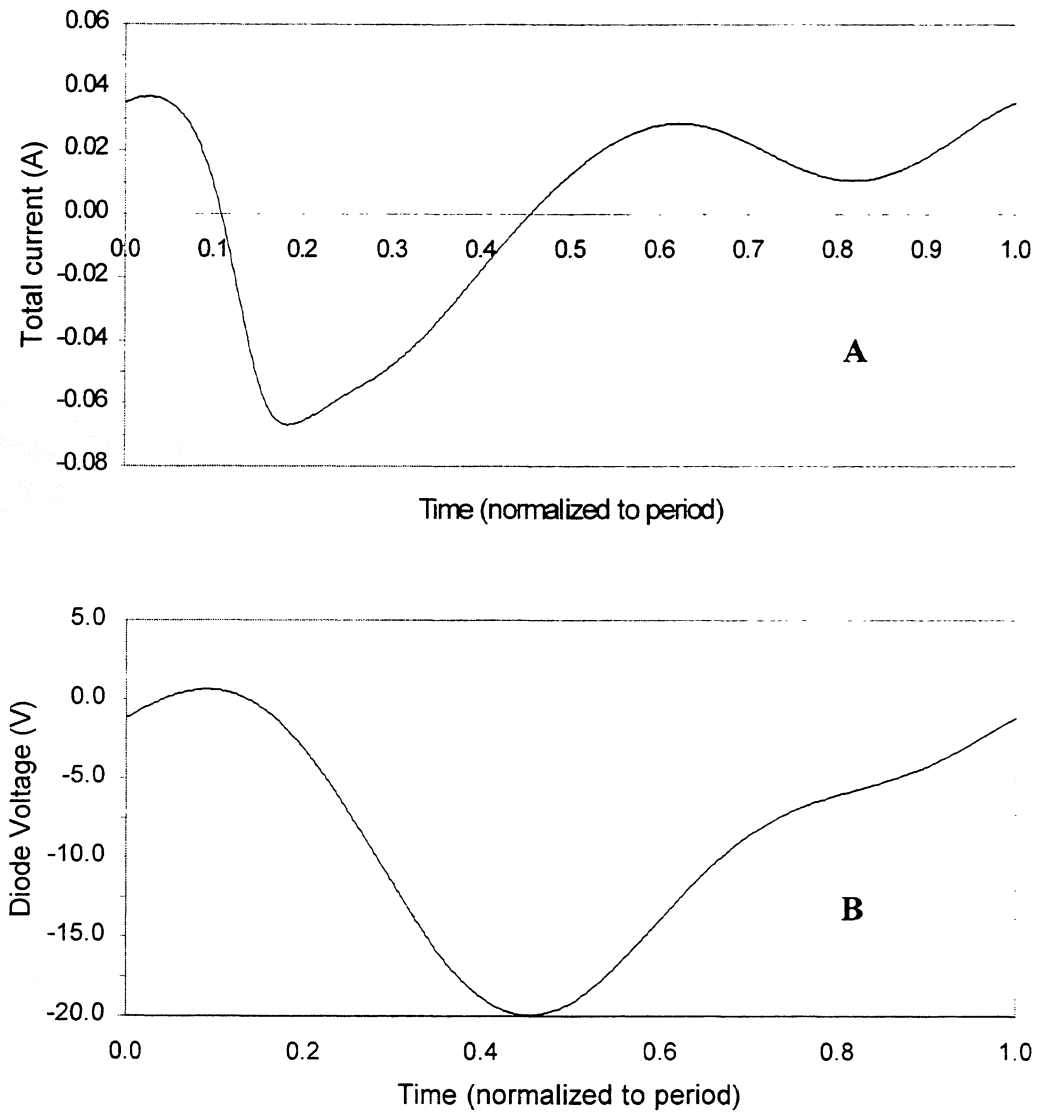**Figure 3.** (A) electron density , and (B) electron temperature, versus position and time.

Figure 4. Large signal , (A) diode current density, (B) diode voltage derived from the hydrodynamic transport model.

for the time-dependent current and voltage waveforms of the UVA-6P4 diode, derived by the hydrodynamic model, are in very good agreement with those obtained from the Monte Carlo harmonic-balance simulator given in reference [7]. As shown in Fig. 4, the peak current density at the optimal power point was approximately *-0.06* amps. This peak value and the overall large-signal current-density characteristic are in almost exact agreement with the MCHB results from [7]. Conversely, the peak value in the large-signal voltage reported here is just below the breakdown value of *20* volts and this is significantly larger the value *~15* volts reported in [7]. It should be noted that the earlier studies in [7] used a constant dc bias voltage did not optimize over the dc bias voltage as was done here (i.e., optimal $V_{DQ} = -8.6$). Hence, our preliminary conclusion is that the previous studies given in [7] did not arrive at the absolute optimal results. This is supported by the difference in embedding impedances for the two studies given in Table II-A and Table II-B. Future simulation studies are planned to resolve the issue of the absolute optimal biasing and embedding for this doubler design.

IV. CONCLUSIONS

This paper has applied a hydrodynamic transport model and a modified harmonic-balance algorithm to the problem of Schottky diode multiplier optimization. The results for a 100/200 doubler study have be compared to an earlier investigation that utilized Monte Carlo and Drift-Diffusion based harmonic-balance algorithms. These results show that this approach can be used to realize improved multiplier operation with a minimal expense of numerical computation. This model will be used in the future to optimize multiplier operation at terahertz frequencies. The physical model and optimization algorithm will be very important to integrated device design that seeks to optimize harmonic-power generation at very high frequencies.

ACKNOWLEDGEMENT

References.

[1]   H. Hjelmgren , "Numerical Modeling of Hot Electrons in n-GaAs Schottky-Barrier Diodes," *IEEE Transactions on Electron Devices*, **37**, pp. 1228-1234 (1990).

[2]   J. O. Nylander, F.Masszi, S. Selberherr and S. Berg , "Computer Simulations of Schottky Contacts with a Non-Constant Recombination Velocity," *Solid State Electronics*, **32**, pp. 363-367 (1989).

[3]   S. A. Maas, *Nonlinear Microwave Circuits*, (Artech House, MA,1988).

[4]   G. B. Tait, "Efficient Solution Method for Unified Nonlinear Microwave Circuit and Numerical Solid-State Device Simulation," *IEEE Microwave Guided Wave Letters*, **4**, pp. 420–422, December (1994).

[5]   P. H. Siegel, A. R. Kerr, and W. Hwang, "Topics in the Optimization of Millimeter-Wave Mixers," *NASA Technical Papers*, no. 2287, March (1984).

[6]   M. T. Faber, J. Chramies and M. E. Adamski, *Microwave and Millimeter-Wave Diode Frequency Multipliers*, (Artech House, MA, 1995).

[7]   R. E. Lipsey, S. H. Jones, J. R. Jones, T. W. Crowe, L. F. Horvath, U. V. Bhapkar, and R. J. Mattauch, "Monte Carlo Harmonic-Balance and Drift-Diffusion Harmonic-Balance Analysis of 100-600 GHz Schottky Barrier Varactor Frequency Multipliers," *IEEE Transactions on Electron Devices*, **44**, pp. 1843-1850 (1997).

[8]   B. L. Gelmont, D. L. Woolard, J. L. Hesler, and T. W. Crowe, "A Degenerately-Doped GaAs Schottky Diode Model Applicable to Terahertz Frequency Regime Operation," *IEEE Transactions on Electron Devices*, **45**, pp. 2521-2527, December (1998).

[9]   D. L. Woolard, B. L. Gelmont, J. L. Hesler and T. W. Crowe, "Physical Aspects of GaAs Schottky Diode Operation at Terahertz Frequency," in Proceedings to 1997 International Device Research Symposium, December 10-13, The University of Virginia, Charlottesville (1997).